

# Subgroup-specific structural variation across 1,000 medulloblastoma genomes

A list of authors and their affiliations appears at the end of the paper

**Medulloblastoma, the most common malignant paediatric brain tumour, is currently treated with nonspecific cytotoxic therapies including surgery, whole-brain radiation, and aggressive chemotherapy. As medulloblastoma exhibits marked intertumoural heterogeneity, with at least four distinct molecular variants, previous attempts to identify targets for therapy have been underpowered because of small samples sizes. Here we report somatic copy number aberrations (SCNAs) in 1,087 unique medulloblastomas. SCNAs are common in medulloblastoma, and are predominantly subgroup-enriched. The most common region of focal copy number gain is a tandem duplication of *SNCAIP*, a gene associated with Parkinson's disease, which is exquisitely restricted to Group 4a. Recurrent translocations of *PVT1*, including *PVT1-MYC* and *PVT1-NDRGI*, that arise through chromothripsis are restricted to Group 3. Numerous targetable SCNAs, including recurrent events targeting TGF- $\beta$  signalling in Group 3, and NF- $\kappa$ B signalling in Group 4, suggest future avenues for rational, targeted therapy.**

Brain tumours are the most common cause of childhood oncological death, and medulloblastoma is the most common malignant paediatric brain tumour. Current medulloblastoma therapy including surgical resection, whole-brain and spinal cord radiation, and aggressive chemotherapy supplemented by bone marrow transplant yields five-year survival rates of 60–70%<sup>1</sup>. Survivors are often left with significant neurological, intellectual and physical disabilities secondary to the effects of these nonspecific cytotoxic therapies on the developing brain<sup>2</sup>.

Recent evidence suggests that medulloblastoma actually comprises multiple molecularly distinct entities whose clinical and genetic differences may require separate therapeutic strategies<sup>3–6</sup>. Four principal subgroups of medulloblastoma have been identified: WNT, SHH, Group 3 and Group 4 (ref. 7), and there is preliminary evidence for clinically significant subdivisions of the subgroups<sup>3,7,8</sup>. Rational, targeted therapies based on genetics are not currently in use for medulloblastoma, although inhibitors of the Sonic Hedgehog pathway protein Smoothed have shown early promise<sup>9</sup>. Actionable targets for WNT, Group 3 and Group 4 tumours have not been identified<sup>4,10</sup>. Sanger sequencing of 22 medulloblastoma exomes revealed on average only 8 single nucleotide variants (SNVs) per tumour<sup>11</sup>. Some SNVs were subgroup-restricted (*PTCH1*, *CTNNB1*), whereas others occurred across subgroups (*TP53*, *MLL2*). We proposed that the observed intertumoural heterogeneity might have underpowered prior attempts to discover targets for rational therapy.

The Medulloblastoma Advanced Genomics International Consortium (MAGIC) consisting of scientists and physicians from 46 cities across the globe gathered more than 1,200 medulloblastomas which were studied by SNP arrays ( $n = 1,239$ ; Fig. 1a, Supplementary Fig. 1 and Supplementary Tables 1–3). Medulloblastoma subgroup affiliation of 827 cases was determined using a custom nanoString-based RNA assay (Supplementary Fig. 2)<sup>12</sup>. Disparate patterns of broad cytogenetic gain and loss were observed across the subgroups (Fig. 1b and Supplementary Figs 3, 7, 8, 10 and 11). Analysis of the entire cohort using GISTIC2 (ref. 13) to discover significant 'driver' events delineated 62 regions of recurrent SCNA (Fig. 1c, Supplementary Fig. 4 and Supplementary Tables 4 and 5); analysis by subgroup increased sensitivity such that 110 candidate 'driver' SCNAs were identified, most of which are subgroup-enriched (Fig. 1c–e and Supplementary Table 6).

Twenty-eight regions of recurrent high-level amplification (copy number  $\geq 5$ ) were identified (Fig. 1d and Supplementary Table 7). The most prevalent amplifications affected members of the MYC family with *MYCN* predominantly amplified in SHH and Group 4, *MYC* in Group 3, and *MYCL1* in SHH medulloblastomas. Multiple genes/regions were exclusively amplified in SHH, including *GLI2*, *MYCL1*, *PPM1D*, *YAP1* and *MDM4* (Fig. 1d). Recurrent homozygous deletions were exceedingly rare, with only 15 detected across 1,087 tumours (Fig. 1e). Homozygous deletions targeting known tumour suppressors *PTEN*, *PTCH1* and *CDKN2A/B* were the most common, all enriched in SHH cases (Fig. 1e and Supplementary Table 7). Novel homozygous deletions included *KDM6A*, a histone-lysine demethylase deleted in Group 4. A custom nanoString CodeSet was used to verify 24 significant regions of gain across 192 MAGIC cases, resulting in a verification rate of 90.9% (Supplementary Fig. 5). We conclude that SCNAs in medulloblastoma are common, and are predominantly subgroup-enriched.

## Subgroup-specific SCNAs in medulloblastoma

WNT medulloblastoma genomes are impoverished of recurrent focal regions of SCNA, exhibiting no significant regions of deletion and only a small subset of focal gains found at comparable frequencies in non-WNT tumours (Supplementary Figs 4, 6 and Supplementary Table 8). *CTNNB1* mutational screening confirmed canonical exon 3 mutations in 63 out of 71 (88.7%) WNT tumours, whereas monosomy 6 was detected in 58 out of 76 (76.3%) (Supplementary Fig. 6; Supplementary Table 9). Four WNT tumours (4/71; 5.6%) had neither *CTNNB1* mutation nor monosomy 6, but maintained typical WNT expression signatures. Given the size of our cohort and the resolution of the platform, we conclude that there are no frequent, targetable SCNAs for WNT medulloblastoma.

SHH tumours exhibit multiple significant focal SCNAs (Fig. 2a, Supplementary Figs 12, 15, 16 and Supplementary Tables 10 and 11). SHH enriched/restricted SCNAs included amplification of *GLI2* and deletion of *PTCH1* (Fig. 2a, e, f)<sup>10</sup>. *MYCN* and *CCND2* were among the most frequently amplified genes in SHH (Supplementary Table 6), but were also altered in non-SHH cases. Genes upregulated in SHH tumours (that is, SHH signature genes) are significantly over-represented among the genes focally amplified in SHH tumours

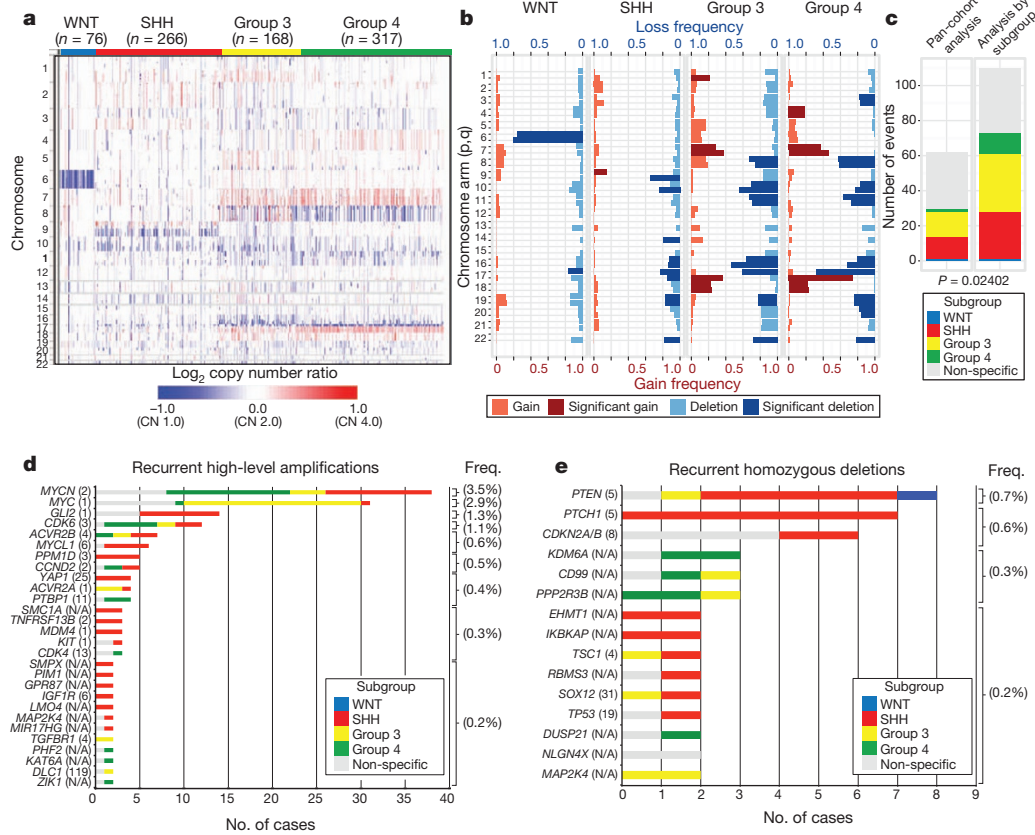


**Figure 1 | Genomic heterogeneity of medulloblastoma subgroups.** **a**, The medulloblastoma genome classified by subgroup. **b**, Frequency and significance ( $Q$  value  $\leq 0.1$ ) of broad cytogenetic events across medulloblastoma subgroups. **c**, Significant regions of focal SCNA identified by GISTIC2 in either pan-cohort or subgroup-specific analyses. **d, e**, Recurrent high-level amplifications ( $d$ , segmented copy number (CN)  $\geq 5$ ) and homozygous deletions ( $e$ , segmented CN  $\leq 0.7$ ) in medulloblastoma. The number of genes mapping to the GISTIC2 peak region (where applicable) is listed in brackets after the suspected driver gene, as is the frequency of each event.

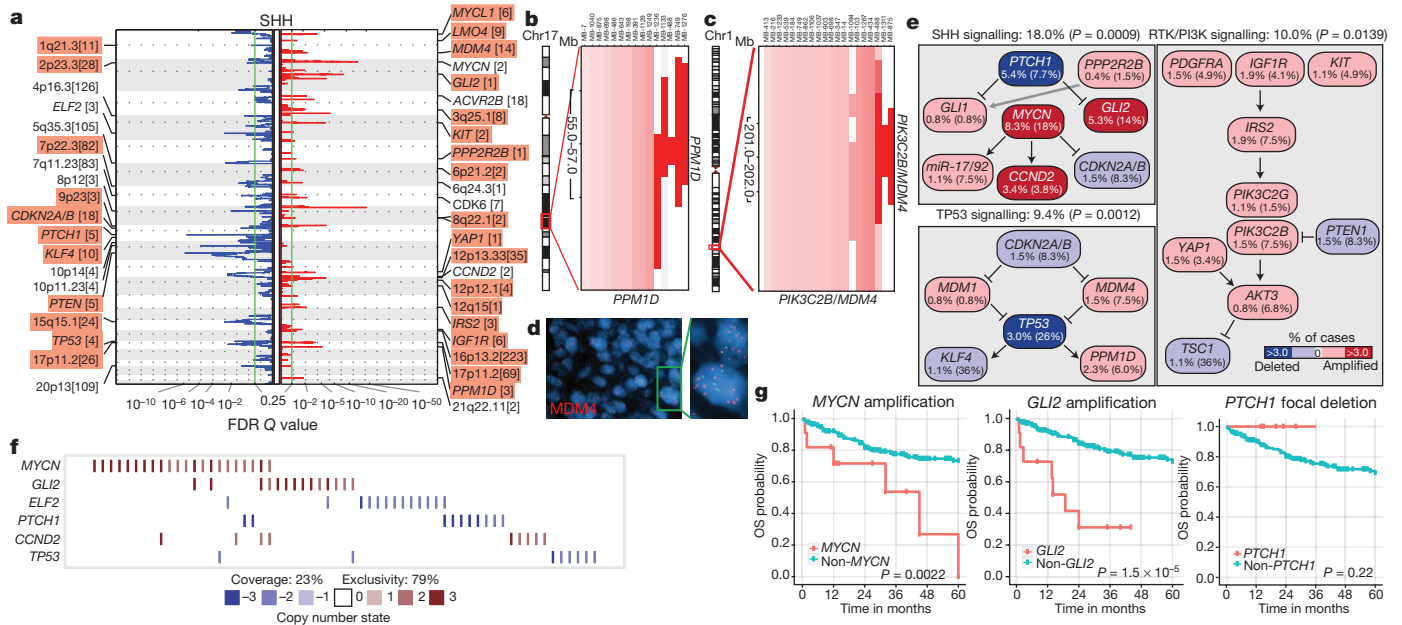


**Figure 2 | Genomic alterations affect core signalling pathways in SHH medulloblastoma.** **a**, GISTIC2 significance plot of amplifications (red) and deletions (blue) observed in SHH. The number of genes mapping to each significant region are included in brackets and regions enriched in SHH are shaded red. **b, c**, Recurrent amplifications of *PPM1D* (**b**) and *PIK3C2B/MDM4* (**c**) are restricted to SHH. **d**, Fluorescence *in situ* hybridization (FISH) validation of *MDM4* amplification. **e**, SHH signalling, TP53 signalling and RTK/PI3K signalling represent the core pathways genomically targeted in SHH.  $P$  values indicate the prevalence with which the respective pathway is targeted in SHH versus non-SHH cases (Fisher's exact test). Frequencies of focal and broad (parentheses) SCNAs are listed. **f**, Mutual exclusivity analysis of focal SCNAs in SHH. **g**, Clinical implications of SCNAs affecting *MYCN*, *GLI2* or *PTCH1* in SHH (log-rank tests).

( $P = 0.001-0.02$ , permutation tests; Supplementary Fig. 9). Recurrent amplification of SHH signature genes has clinical implications, as amplification of downstream transcriptional targets could mediate resistance to upstream SHH pathway inhibitors<sup>14</sup>.

Novel, SHH-enriched SCNAs included components of TP53 signalling, including amplifications of *MDM4* and *PPM1D*, and focal deletions of *TP53* (Fig. 2a–e). Targetable events, including amplifications of IGF signalling genes *IGF1R* and *IRS2*, PI3K genes *PIK3C2G* and *PIK3C2B*, and deletion of *PTEN* were restricted to SHH tumours (Fig. 2a, c, e). Importantly, focal events affecting genes in the SHH pathway were largely mutually exclusive and prognostically significant (Fig. 2f, g). Many of the recurrent, targetable SCNAs identified in SHH medulloblastoma (*IGF1R*, *KIT*, *MDM4*, *PDGFRA*, *PIK3C2G*, *PIK3C2B* and *PTEN*) have already been targeted with small molecules for treatment of other malignancies, which might allow rapid translation for targeted therapy of subsets of SHH patients (Supplementary Table 16). Novel SHH targets identified here are excellent candidates for combinatorial therapy with Smoothed inhibitors, to avoid the resistance encountered in both humans and mice<sup>9,14,15</sup>.

Group 3 and Group 4 medulloblastomas have generic names as comparatively little is known about their genetic basis, and no targets for rational therapy have been identified<sup>7</sup>. *MYC* amplicons are largely restricted to Group 3, whereas *MYCN* amplicons are seen in Group 4 and SHH tumours (Fig. 1d)<sup>3,4</sup>. Indeed, *MYC* and *MYCN* loci comprise the most significant regions of amplification observed in Group 3 and Group 4, respectively (Fig. 3a, b, Supplementary Figs 13, 14, 17–20 and Supplementary Tables 12–15). Group 3 *MYC* amplicons were mutually exclusive from those affecting the known medulloblastoma oncogene *OTX2* (ref. 16) and were highly prognostic (Supplementary Fig. 21)<sup>3,16</sup>. Type II activin receptors, *ACVR2A* and *ACVR2B* and family member *TGFBR1* are highly amplified in Group 3 tumours, indicating deregulation of TGF- $\beta$  signalling as a driver event in Group 3 (Fig. 3c–e and Supplementary Fig. 22). The Group 3-enriched

medulloblastoma oncogene *OTX2* is a prominent target of TGF- $\beta$  signalling in the developing nervous system<sup>17</sup> and TGF- $\beta$  pathway inhibitors *CD109* (ref. 18), *FKBP1A* (refs 19 and 20) and *SNX6* (ref. 20) are recurrently deleted in Group 3 (Fig. 3a, d). SCNAs in TGF- $\beta$  pathway genes were heavily enriched in Group 3 ( $P = 5.37 \times 10^{-5}$ , Fisher's exact test) and found in at least 20.2% of cases, indicating that TGF- $\beta$  signalling represents the first rational target for this poor prognosis subgroup (Fig. 3d). Similarly, novel deletions affecting regulators of the NF- $\kappa$ B pathway, including *NFKBIA* (ref. 21) and *USP4* (ref. 22) were identified in Group 4 (Supplementary Fig. 23), proposing that NF- $\kappa$ B signalling may represent a rational Group 4 therapeutic target.

Network analysis of Group 3 and Group 4 SCNAs illustrates the different pathways over-represented in each subgroup. Only TGF- $\beta$  signalling is unique to Group 3 (Fig. 3e). In contrast, cell-cycle control, chromatin modification and neuronal development are all Group 4-enriched. Cumulatively, the dismal prognosis of Group 3 patients, the lack of published targets for rational therapy, and the prior targeting of TGF- $\beta$  signalling in other diseases suggest that TGF- $\beta$  may represent an appealing target for Group 3 rational therapies (Supplementary Table 16).

### SNCAIP tandem duplication is common in Group 4

Although Group 4 is the most prevalent medulloblastoma subgroup, its pathogenesis remains poorly understood. The most frequent SCNA observed in Group 4 (33/317; 10.4%) is a recurrent region of single copy gain on chr5q23.2 targeting a single gene, *SNCAIP* (synuclein, alpha interacting protein) (Fig. 4a and Supplementary Fig. 24). *SNCAIP*, encodes synphilin-1, which binds to  $\alpha$ -synuclein to promote the formation of Lewy bodies in the brains of patients with Parkinson's disease<sup>23,24</sup>. Additionally, rare germline mutations of *SNCAIP* have been described in Parkinson's families<sup>25</sup>. Large insert, mate-pair, whole-genome sequencing (WGS) demonstrates that

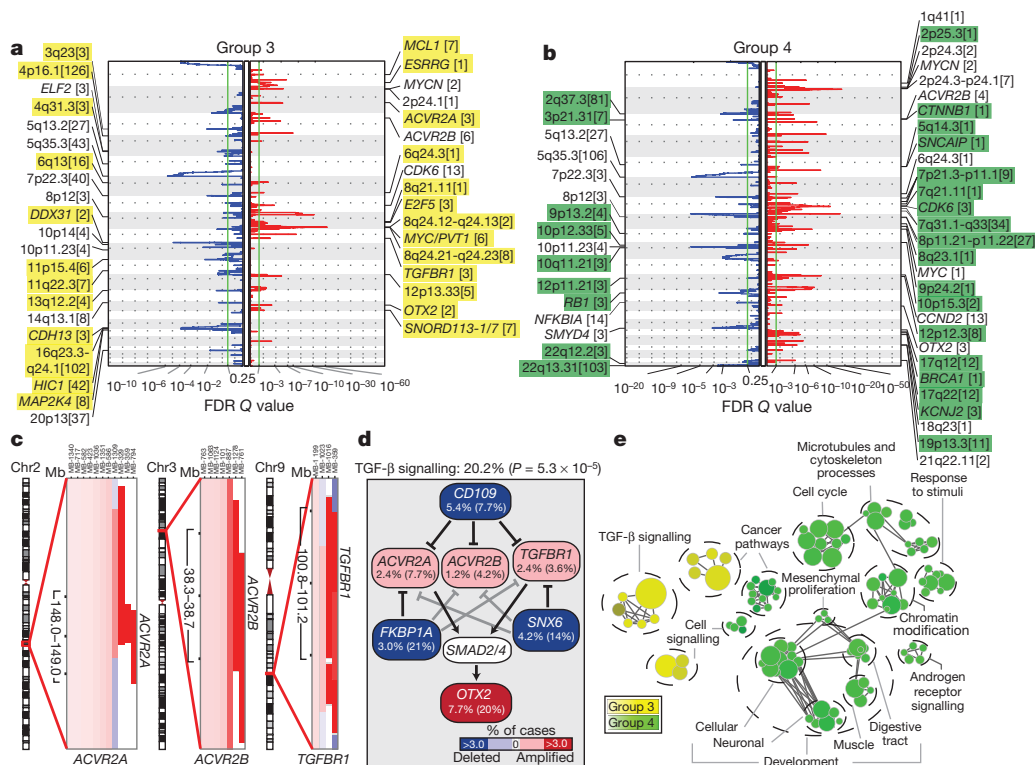


**Figure 3 | The genomic landscape of Group 3 and Group 4 medulloblastoma.** a, b, GISTIC2 plots depicting significant SCNAs in Group 3 (a) and Group 4 (b) with subgroup-enriched regions shaded in yellow and green, respectively. c, Recurrent amplifications targeting type II (*ACVR2A* and

*ACVR2B*) and type I (*TGFBR1*) activin receptors in Group 3. d, Recurrent SCNAs affecting the TGF- $\beta$  pathway in Group 3 ( $P = 5.73 \times 10^{-5}$ , Fisher's exact test). Frequencies of focal and broad (parentheses) SCNAs are listed. e, Enrichment map of gene sets affected by SCNAs in Group 3 versus Group 4.



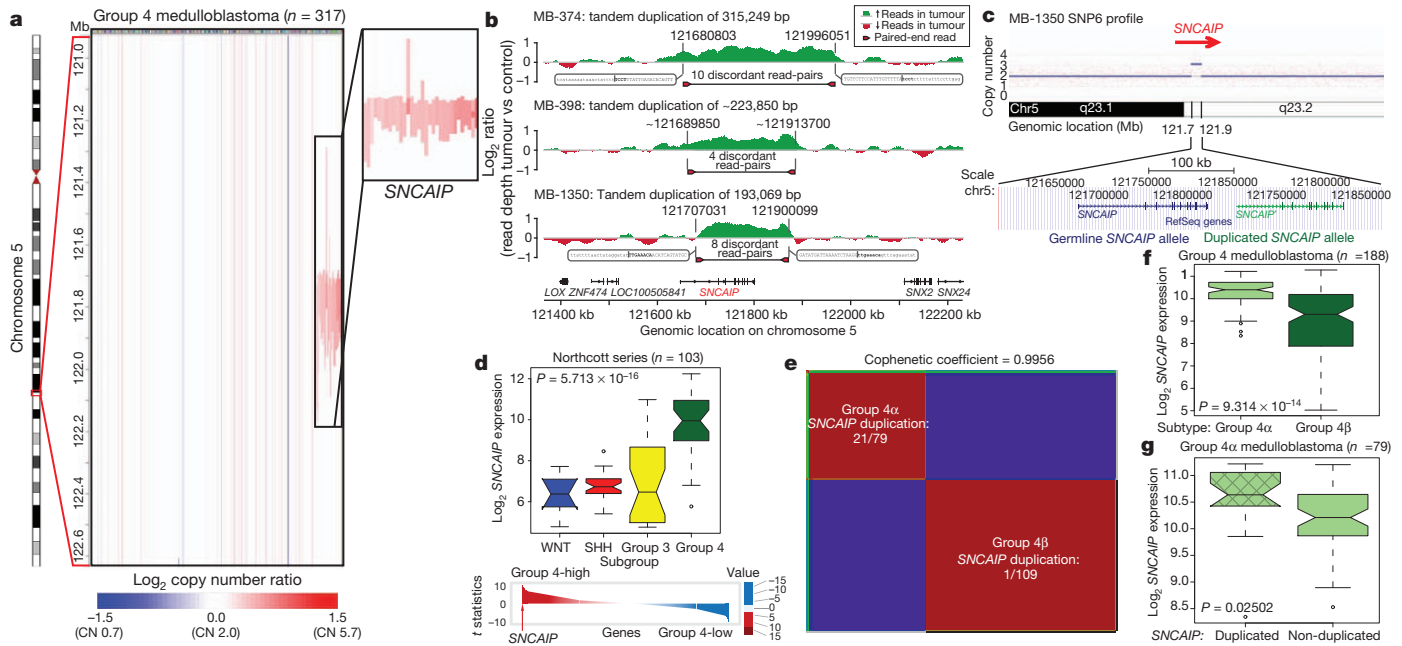


**Figure 4 | Tandem duplication of *SNCAIP* defines a novel subtype of Group 4.** **a**, Highly recurrent, focal, single-copy gain of *SNCAIP* in Group 4. **b**, Paired-end mapping verifies recurrent tandem duplication of *SNCAIP* in Group 4. **c**, Schematic representation of *SNCAIP* tandem duplication. **d**, *SNCAIP* is a Group 4 signature gene. Upper panel, *SNCAIP* expression across subgroups in a published series of 103 primary medulloblastomas. Error bars depict the minimum and maximum values, excluding outliers. Lower panel, *SNCAIP* ranks among the top 1% (rank, 39th out of 16,758) of highly expressed genes in

Group 4. **e**, NMF consensus clustering of 188 expression-profiled Group 4 tumours supports two transcriptionally distinct subtypes designated 4 $\alpha$  and 4 $\beta$  (cophenetic coefficient = 0.9956). 21 out of 22 *SNCAIP* duplicated cases belong to Group 4 $\alpha$  ( $P = 3.12 \times 10^{-8}$ , Fisher's exact test). **f**, *SNCAIP* expression is significantly elevated in Group 4 $\alpha$  versus 4 $\beta$  ( $P = 9.31 \times 10^{-14}$ , Mann-Whitney test). **g**, Group 4 $\alpha$  cases harbouring *SNCAIP* duplication exhibit a ~1.5-fold increase in *SNCAIP* expression. **f**, **g**, Error bars depict the minimum and maximum values, excluding outliers.

*SNCAIP* copy number gains arise from tandem duplication of a truncated *SNCAIP* (lacking non-coding exon 1), inserted telomeric to the germline *SNCAIP* allele (Fig. 4b, c and Supplementary Fig. 25). Affymetrix SNP6 array profiling of patient-matched germline material confirmed that *SNCAIP* duplications are somatic (Supplementary Fig. 26), and subsequent whole-transcriptome sequencing (RNA-Seq) of select Group 4 cases ( $n = 5$ ) verified that *SNCAIP* is the only gene expressed in the duplicated region (Supplementary Fig. 27). Analysis of published copy number profiles for 3,131 primary tumours<sup>26</sup> and 947 cancer cell lines<sup>27</sup> (total of 4,078 cases) revealed only four cases with apparent duplication of *SNCAIP*, all of which were inferred as Group 4 medulloblastomas (data not shown). We conclude that *SNCAIP* duplication is a somatic event highly specific to Group 4 medulloblastoma.

Re-analysis of 499 published medulloblastoma expression profiles confirmed that *SNCAIP* is one of the most highly upregulated Group 4 signature genes (Fig. 4d and Supplementary Fig. 28). Profiling of 188 Group 4 tumours on expression microarrays followed by consensus non-negative matrix factorization (NMF) clustering delineates two subtypes of Group 4 (4 $\alpha$  and 4 $\beta$ ; Fig. 4e and Supplementary Fig. 29). Strikingly, 21 out of 22 *SNCAIP* duplicated cases belonged to Group 4 $\alpha$  ( $P = 3.12 \times 10^{-8}$ , Fisher's exact test). *SNCAIP* is more highly expressed in Group 4 $\alpha$  than 4 $\beta$  (Fig. 4f), and 4 $\alpha$  samples with tandem duplication showed approximately 1.5-fold increased expression, consistent with gene dosage (Fig. 4g and Supplementary Figs 35 and 36). Group 4 $\alpha$  exhibits a relatively balanced genome compared to 4 $\beta$  (Supplementary Figs 30–32), and several 4 $\alpha$  cases harbour *SNCAIP* duplication in conjunction with i17q and no other SCNAs (Supplementary Fig. 33). Importantly, *SNCAIP* duplications are mutually exclusive from other prominent SCNAs in Group 4, including *MYCN* and *CDK6* amplifications (Supplementary Fig. 34).

### PVT1 fusions arise via chromothripsis in Group 3

Although recurrent gene fusions have recently been discovered in solid tumours, none have been reported in medulloblastoma. RNA-Seq of

Group 3 tumours ( $n = 13$ ) identified two independent gene fusions in two different tumours (MB-182 and MB-586), both involving the 5' end of *PVT1*, a non-coding gene frequently co-amplified with *MYC* in Group 3 (Fig. 5a, b, Supplementary Fig. 37 and Supplementary Tables 17 and 18). Sanger sequencing confirmed a fusion transcript consisting of exons 1 and 3 of *PVT1* fused to the coding sequence of *MYC* (exons 2 and 3) in MB-182, and a fusion involving *PVT1* exon 1 fused to the 3' end of *NDRG1* in MB-586 (Fig. 5a, b).

Group 3 copy number data at the *MYC/PVT1* locus indicated that additional samples might harbour *PVT1* gene fusions (Fig. 5c). PCR with reverse transcription (RT-PCR) profiling of select Group 3 cases confirmed *PVT1-MYC* fusions in at least 60% (12/20) of *MYC*-amplified cases (Fig. 5d and Supplementary Table 19). Fusion transcripts included many other portions of chr8q, with up to four different genomic loci mapping to a single transcript, a pattern reminiscent of chromothripsis<sup>28,29</sup> (Fig. 5d). WGS performed on four *MYC*-amplified Group 3 tumours harbouring *PVT1* fusion transcripts identified a series of complex genomic rearrangements on chr8q (Fig. 5e, f, Supplementary Fig. 38 and Supplementary Tables 20 and 21). Chromosome 8 copy number profile for MB-586 (*PVT1-NDRG1*) derived from WGS showed that *PVT1* and *NDRG1* are structurally linked, as predicted by RNA-Seq, and several adjacent regions of 8q24 were extensively rearranged (Fig. 5e, f and Supplementary Table 21). Monte Carlo simulation suggests that this fragmented 8q amplicon arose through chromothripsis, a process of erroneous DNA repair following a single catastrophic event in which a chromosome is shattered into many pieces (Supplementary Fig. 39). Further examination of our copy number data set revealed rare examples of chromothripsis across subgroups (Supplementary Fig. 40), with only chr8 in Group 3 demonstrating statistically significant, region-specific chromothripsis ( $Q = 0.0004$ , false discovery rate (FDR)-corrected Fisher's exact test). Among Group 3 tumours, the occurrence of chr8q chromothripsis is correlated with deletion of chr17p (location of *TP53*; data not shown), in keeping with the association of loss of

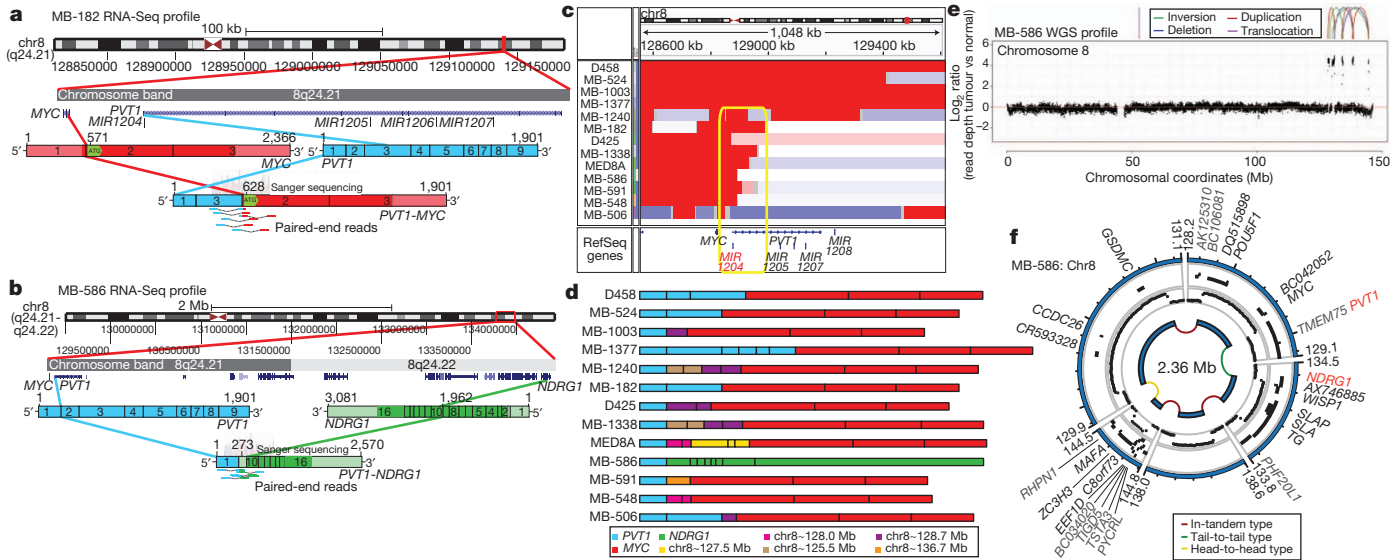


**Figure 5 | Identification of frequent *PVT1*-*MYC* fusion genes in Group 3.** **a, b**, RNA-Seq identifies multiple fusion transcripts driven by *PVT1* in Group 3. Schematics depict the structures of verified *PVT1*-*MYC* (**a**) and *PVT1*-*NDRG1* (**b**) fusion genes. **c**, Heat map of the *MYC*/*PVT1* locus showing a subset of 13 *MYC*-amplified Group 3 cases subsequently verified to exhibit *PVT1* gene

fusions (shown in **d**). Yellow box highlights the common breakpoint affecting the first exon/intron of *PVT1*, including *miR-1204*. **d**, Summary of *PVT1* fusion transcripts identified in Group 3. **e, f**, WGS confirms complex patterns of rearrangement on chr8q24 in *PVT1* fusion (+) Group 3.

*TP53* and chromothripsis recently described in medulloblastoma ( $P = 0.0199$ , Fisher's exact test)<sup>28</sup>. Whereas the *PVT1* locus has been suggested to be a genomically fragile site, we observe that the majority of *MYC*-amplified Group 3 tumours harbour *PVT1* fusions that arise through a process consistent with chromothripsis.

*PVT1* is a non-coding host gene for four microRNAs, *miR-1204*-*miR-1207*. Previous studies have implicated *miR-1204* as a candidate oncogene that enhances oncogenesis in combination with *MYC*<sup>30,31</sup>. *PVT1* fusions identified in this study involve only *PVT1* exon 1 and *miR-1204*. Importantly, *miR-1204*, but not the adjacent *miR-1205* and *miR-1206*, is expressed at a higher level in *PVT1*-*MYC* fusion (+) Group 3 tumours compared to fusion (-) cases ( $P = 0.0008$ , Mann-Whitney test; Fig. 6a). To evaluate whether aberrant expression of *miR-1204* contributes to the malignant phenotype, we inhibited *miR-1204* in MED8A cells, a Group 3 medulloblastoma cell line with a confirmed *PVT1*-*MYC* fusion (Fig. 5d). Antagomir-mediated RNA

interference of *miR-1204* had a pronounced effect on MED8A growth (Fig. 6b). A comparable reduction in proliferative capacity was achieved with knockdown of *MYC*. Conversely, the medulloblastoma cell line ONS76 exhibits neither *MYC* amplification nor a detectable *PVT1*-*MYC* fusion gene, and knockdown of *miR-1204* had no effect in this line (Fig. 6c).

*PVT1* has been reported previously in fusion transcripts with a number of partners<sup>30,32,33</sup>. The most prevalent form of the *PVT1*-*MYC* fusion in Group 3 tumours lacks the first, non-coding exon of *MYC*, similar to forms of *MYC* that have been described in Burkitt's lymphoma<sup>34</sup> (Fig. 5a, d). The *PVT1* promoter contains two non-canonical E-boxes and can be activated by *MYC*<sup>31</sup>. This indicates a positive feedback model where *MYC* can reinforce its own expression from the *PVT1* promoter in *PVT1*-*MYC* fusion (+) tumours. Indeed, knockdown of *MYC* alone in MED8A cells resulted in diminished expression of both *MYC* and *miR-1204*, suggesting *MYC* may positively regulate *PVT1* (that is, *miR-1204*) expression in medulloblastoma cells (Supplementary Fig. 41).

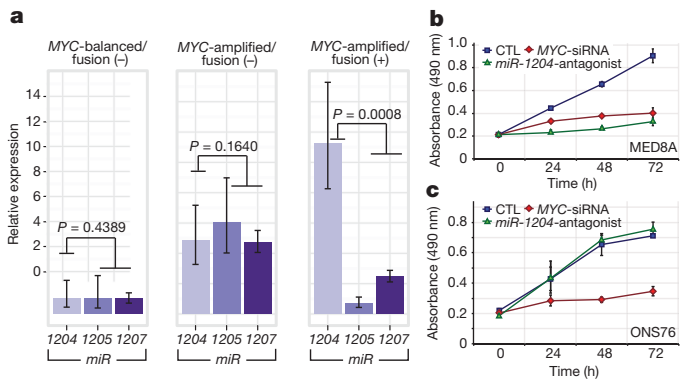


**Figure 6 | Functional synergy between *miR-1204* and *MYC* secondary to *PVT1*-*MYC* fusion.** **a**, Quantitative RT-PCR of *PVT1*-encoded microRNAs confirms upregulation of *miR-1204* in *PVT1*-*MYC* fusion (+) Group 3 tumours. *MYC*-balanced/fusion (-),  $n = 4$ ; *MYC*-amplified/fusion (-),  $n = 6$ ; *MYC*-amplified/fusion (+),  $n = 8$ . Error bars represent standard error of the mean (s.e.m.) and reflect variability among samples. **b, c**, Knockdown of *miR-1204* attenuates the proliferative capacity of *PVT1*-*MYC* fusion (+) MED8A medulloblastoma cells (**b**) but has no effect on fusion (-) ONS76 cells (**c**). Error bars represent the standard deviation (s.d.) of triplicate experiments. CTL, control.

**Discussion**

Medulloblastomas have few SNVs compared to many adult epithelial malignancies<sup>11</sup>, whereas SCNAs seem to be quite common. Medulloblastoma is a heterogeneous disease<sup>7</sup>, thereby requiring large cohorts to detect subgroup-specific events. Through the accumulation of >1,200 medulloblastomas in MAGIC, we have identified novel and significant SCNAs. Many of the significant SCNAs are subgroup-restricted, highly supporting their role as driver events in their respective subgroups.

Expression of synphilin-1 in neuronal cells results in decreased cell doubling time<sup>35</sup>, decreased caspase-3 activation<sup>36</sup>, decreased *TP53* transcriptional activity and messenger RNA levels, and decreased apoptosis<sup>37</sup>. Synphilin-1 is ubiquitinated by parkin, which is encoded by the hereditary Parkinson's disease gene *PARK2* (ref. 24), a candidate tumour suppressor gene<sup>38</sup>. Whereas patients with Parkinson's disease have an overall decreased risk of cancer, they may have an increased incidence of brain tumours<sup>39,40</sup>. As tandem duplications of *SNCAIP* are highly recurrent, stereotypical, subgroup-restricted, affect only a single gene, and as *SNCAIP*-duplicated tumours have few if any other SCNAs, *SNCAIP* is a probable driver gene, and merits investigation

as a target for therapy of Group 4a. Similarly, *PVT1* fusion genes are highly recurrent, restricted to Group 3, arise through a chromothripsis-like process, and are the first recurrent translocation reported in medulloblastoma.

We identify a number of highly targetable, recurrent, subgroup-specific SCNAs that could form the basis for future clinical trials (that is, PI3K signalling in SHH, TGF- $\beta$  signalling in Group 3, and NF- $\kappa$ B signalling in Group 4). Activation of these pathways through alternative, currently unknown genetic and epigenetic events could increase the percentage of patients amenable to targeted therapy. We also identify a number of highly 'druggable' events that occur in a minority of cases. The cooperative, global approach of the MAGIC consortium has allowed us to overcome the barrier of intertumoural heterogeneity in an uncommon paediatric tumour, and to identify the relevant and targetable SCNAs for the affected children.

## METHODS SUMMARY

All patient samples were obtained with consent as outlined by individual institutional review boards. Genomic DNA was prepared, processed and hybridized to Affymetrix SNP6 arrays according to manufacturer's instructions. Raw copy number estimates were obtained in dChip, followed by CBS segmentation in R. SCNAs were identified using GISTIC2 (ref. 13). Driver genes within SCNAs were inferred by integrating matched expressions, literature evidence and other data sets. Pathway enrichment of SCNAs was analysed with g:Profiler and visualized in Cytoscape using Enrichment Map. Fluorescence *in situ* hybridization (FISH) was performed as described previously<sup>8,10</sup>. Medulloblastoma subgroup was assigned using a custom nanoString CodeSet as described previously<sup>12</sup>. Tandem duplication of *SNCAIP* was confirmed by paired-end mapping as previously reported<sup>28</sup>. RNA was extracted, processed and hybridized to Affymetrix Gene 1.1 ST Arrays as recommended by the manufacturer. Consensus NMF clustering was performed in GenePattern. Gene fusions were identified from RNA-Seq data using Trans-ABYSS. Medulloblastoma cell lines were maintained as described<sup>10</sup>. Proliferation assays were performed with the Promega CellTiter 96 Assay. Additional methods are detailed in full in Supplementary Methods.

Received 29 February; accepted 14 June 2012.

Published online 25 July 2012.

- Gajjar, A. *et al.* Risk-adapted craniospinal radiotherapy followed by high-dose chemotherapy and stem-cell rescue in children with newly diagnosed medulloblastoma (St Jude Medulloblastoma-96): long-term results from a prospective, multicentre trial. *Lancet Oncol.* **7**, 813–820 (2006).
- Mabbott, D. J. *et al.* Serial evaluation of academic and behavioral outcome after treatment with cranial radiation in childhood. *J. Clin. Oncol.* **23**, 2256–2263 (2005).
- Cho, Y. J. *et al.* Integrative genomic analysis of medulloblastoma identifies a molecular subgroup that drives poor clinical outcome. *J. Clin. Oncol.* **29**, 1424–1430 (2011).
- Northcott, P. A. *et al.* Medulloblastoma comprises four distinct molecular variants. *J. Clin. Oncol.* **29**, 1408–1414 (2011).
- Remke, M. *et al.* *FSTL5* is a marker of poor prognosis in non-WNT/non-SHH medulloblastoma. *J. Clin. Oncol.* **29**, 3852–3861 (2011).
- Northcott, P. A., Korshunov, A., Pfister, S. M. & Taylor, M. D. The clinical implications of medulloblastoma subgroups. *Nature Rev. Neurol.* **8**, 340–351 (2012).
- Taylor, M. D. *et al.* Molecular subgroups of medulloblastoma: the current consensus. *Acta Neuropathol.* **123**, 465–472 (2011).
- Northcott, P. A. *et al.* Pediatric and adult sonic hedgehog medulloblastomas are clinically and molecularly distinct. *Acta Neuropathol.* **122**, 231–240 (2011).
- Rudin, C. M. *et al.* Treatment of medulloblastoma with hedgehog pathway inhibitor GDC-0449. *N. Engl. J. Med.* **361**, 1173–1178 (2009).
- Northcott, P. A. *et al.* Multiple recurrent genetic events converge on control of histone lysine methylation in medulloblastoma. *Nature Genet.* **41**, 465–472 (2009).
- Parsons, D. W. *et al.* The genetic landscape of the childhood cancer medulloblastoma. *Science* **331**, 435–439 (2011).
- Northcott, P. A. *et al.* Rapid, reliable, and reproducible molecular sub-grouping of clinical medulloblastoma samples. *Acta Neuropathol.* **123**, 615–626 (2012).
- Mermel, C. H. *et al.* GISTIC2.0 facilitates sensitive and confident localization of the targets of focal somatic copy-number alteration in human cancers. *Genome Biol.* **12**, R41 (2011).
- Buonamici, S. *et al.* Interfering with resistance to smoothened antagonists by inhibition of the PI3K pathway in medulloblastoma. *Sci. Transl. Med.* **2**, 51ra70 (2010).
- Yauch, R. L. *et al.* Smoothened mutation confers resistance to a hedgehog pathway inhibitor in medulloblastoma. *Science* **326**, 572–574 (2009).
- Adamson, D. C. *et al.* OTX2 is critical for the maintenance and progression of Shh-independent medulloblastomas. *Cancer Res.* **70**, 181–191 (2010).
- Jia, S., Wu, D., Xing, C. & Meng, A. Smad2/3 activities are required for induction and patterning of the neuroectoderm in zebrafish. *Dev. Biol.* **333**, 273–284 (2009).
- Bizet, A. A. *et al.* The TGF- $\beta$  co-receptor, CD109, promotes internalization and degradation of TGF- $\beta$  receptors. *Biochim. Biophys. Acta* **1813**, 742–753 (2011).
- Wang, T., Donahoe, P. K. & Zervos, A. S. Specific interaction of type I receptors of the TGF-beta family with the immunophilin FKBP-12. *Science* **265**, 674–676 (1994).
- Parks, W. T. *et al.* Sorting nexin 6, a novel SNX, interacts with the transforming growth factor- $\beta$  family of receptor serine-threonine kinases. *J. Biol. Chem.* **276**, 19332–19339 (2001).
- Bredel, M. *et al.* *NFKBIA* deletion in glioblastomas. *N. Engl. J. Med.* **364**, 627–637 (2011).
- Xiao, N. *et al.* Ubiquitin-specific protease 4 (USP4) targets TRAF2 and TRAF6 for deubiquitination and inhibits TNF $\alpha$ -induced cancer cell migration. *Biochem. J.* **441**, 979–986 (2012).
- Engelender, S. *et al.* Synphilin-1 associates with  $\alpha$ -synuclein and promotes the formation of cytosolic inclusions. *Nature Genet.* **22**, 110–114 (1999).
- Chung, K. K. *et al.* Parkin ubiquitinates the  $\alpha$ -synuclein-interacting protein, synphilin-1: implications for Lewy-body formation in Parkinson disease. *Nature Med.* **7**, 1144–1150 (2001).
- Marx, F. P. *et al.* Identification and functional characterization of a novel R621C mutation in the synphilin-1 gene in Parkinson's disease. *Hum. Mol. Genet.* **12**, 1223–1231 (2003).
- Beroukhim, R. *et al.* The landscape of somatic copy-number alteration across human cancers. *Nature* **463**, 899–905 (2010).
- Barretina, J. *et al.* The Cancer Cell Line Encyclopedia enables predictive modelling of anticancer drug sensitivity. *Nature* **483**, 603–607 (2012).
- Rausch, T. *et al.* Genome sequencing of pediatric medulloblastoma links catastrophic DNA rearrangements with *TP53* mutations. *Cell* **148**, 59–71 (2012).
- Stephens, P. J. *et al.* Massive genomic rearrangement acquired in a single catastrophic event during cancer development. *Cell* **144**, 27–40 (2011).
- Shtivelman, E. & Bishop, J. M. The *PVT* gene frequently amplifies with *MYC* in tumor cells. *Mol. Cell. Biol.* **9**, 1148–1154 (1989).
- Carramusa, L. *et al.* The *PVT-1* oncogene is a Myc protein target that is overexpressed in transformed cells. *J. Cell. Physiol.* **213**, 511–518 (2007).
- Shtivelman, E. & Bishop, J. M. Effects of translocations on transcription from *PVT*. *Mol. Cell. Biol.* **10**, 1835–1839 (1990).
- Pleasant, E. D. *et al.* A small-cell lung cancer genome with complex signatures of tobacco exposure. *Nature* **463**, 184–190 (2010).
- Hann, S. R., King, M. W., Bentley, D. L., Anderson, C. W. & Eisenman, R. N. A non-AUG translational initiation in *c-myc* exon 1 generates an N-terminally distinct protein whose synthesis is disrupted in Burkitt's lymphomas. *Cell* **52**, 185–195 (1988).
- Li, X. *et al.* Synphilin-1 exhibits trophic and protective effects against Rotenone toxicity. *Neuroscience* **165**, 455–462 (2010).
- Smith, W. W. *et al.* Synphilin-1 attenuates neuronal degeneration in the A53T alpha-synuclein transgenic mouse model. *Hum. Mol. Genet.* **19**, 2087–2098 (2010).
- Giaime, E. *et al.* Caspase-3-derived C-terminal product of synphilin-1 displays antiapoptotic function via modulation of the p53-dependent cell death pathway. *J. Biol. Chem.* **281**, 11515–11522 (2006).
- Veeriah, S. *et al.* Somatic mutations of the Parkinson's disease-associated gene *PARK2* in glioblastoma and other human malignancies. *Nature Genet.* **42**, 77–82 (2010).
- Olsen, J. H. *et al.* Atypical cancer pattern in patients with Parkinson's disease. *Br. J. Cancer* **92**, 201–205 (2005).
- Moller, H., Mellemkjaer, L., McLaughlin, J. K. & Olsen, J. H. Occurrence of different cancers in patients with Parkinson's disease. *Br. Med. J.* **310**, 1500–1501 (1995).

**Supplementary Information** is linked to the online version of the paper at [www.nature.com/nature](http://www.nature.com/nature).

**Acknowledgements** M.D.T. is the recipient of a CIHR Clinician-Scientist Phase II award, and was formerly a Sontag Distinguished Scholar with funds from the Sontag Foundation. Funding is acknowledged from the Pediatric Brain Tumour Foundation (M.D.T. and J.T.R.), and the National Institutes of Health (CA159859 to M.D.T., R.W.R. and B.W.), The Canadian Cancer Society, Genome Canada, Genome BC, Terry Fox Research Institute, Ontario Institute for Cancer Research, Pediatric Oncology Group Ontario, Funds from 'The Family of Kathleen Lorette' and the Clark H. Smith Brain Tumour Centre, Montreal Children's Hospital Foundation, Hospital for Sick Children: Sonia and Arthur Labatt Brain Tumour Research Centre, Chief of Research Fund, Cancer Genetics Program, Garron Family Cancer Centre, B.R.A.I.N. Child, CIHR (grant no. ATE-110814); the University of Toronto McLaughlin Centre, CIHR Institute of Cancer Research (grant no. AT1 – 112286) and C17 through the Advancing Technology Innovation through Discovery competition (Project Title: The Canadian Pediatric Cancer Genome Consortium: Translating next-generation sequencing technologies into improved therapies for high-risk childhood cancer). Canada's Michael Smith Genome Sciences Centre is supported by the BC Cancer Foundation. J.R. is supported by The Children's Discovery Institute. P.A.N. was supported by a Restracomp Fellowship (Hospital for Sick Children) and is currently a Roman-Herzog Postdoctoral Fellow (Hertie Foundation). Salary support for L.G. was provided by the Ontario Institute for Cancer Research through funding provided by the Government of Ontario. E.V.G.M. is supported by NIH grants CA86335, CA116804, CA138292, NCI contracts 28XS100 and 29XS193, the Southeastern Brain Tumour Foundation, and the Brain Tumour Foundation for Children. This study includes samples provided by the UK Children's Cancer and Leukaemia Group (CCLG) as part of CCLG-approved biological study BS-2007-04. J.K. and S.P. were supported by a grant from the German



Cancer Aid (109252). We thank C. Lu, K. Otaka and The Centre for Applied Genomics for technical assistance. We thank N. S. Devi and Z. Zhang for technical assistance. We thank D. Stoll for project management, S. Archer for technical writing, and P. Paroutis for artwork. The MAGIC project is part of the International Cancer Genome Consortium.

**Author Contributions** P.A.N. and M.D.T. co-conceived the study. P.A.N., M.A.M., and M.D.T. led the study. P.A.N. planned and executed experiments and analyses, supervised data acquisition, performed bioinformatic analyses, and extracted nucleic acids for the MAGIC cohort. D.J.H.S. led the bioinformatics and performed analyses. J.P. performed quantitative RT-PCR and Sanger sequencing of *PVT1* fusions, expression profiled *PVT1*-encoded miRNAs, and generated schematics for *PVT1* fusion genes. L.G. performed the *MYC* and *miR-1204* knockdown experiments. A.S.M. supervised the RNA-Seq and WGS experiments and performed data analysis. T.Z., A.M.S. and J.O.K. performed the large insert paired-end sequencing and PCR verification of *SNCAIP* duplication samples. A.Ko. performed interphase FISH and immunohistochemistry for candidate genes. J.R. and G.D.B. led the pathway analyses and generated enrichment plots. S.E.S. and R.B. provided technical support with the GISTIC2 bioinformatic platform. D.W.E. performed interphase FISH for candidate genes. C.R.M., A.C.L. and S.W.S. performed the SNP6 genotyping analysis, provided a database of normal copy number variants, and the control dataset used to infer copy number in the tumour samples. S.M., A.D., F.M.G.C., M.K., D.T.W.J. and H.W. performed bioinformatic analyses and provided technical advice. Y.Y. sequenced *CTNBN1* in the WNT tumours. V.R., D.K., M.F.R., T.A., and P.D. performed functional assays for candidate genes. B.Lu. extracted nucleic acids, managed biobanking, and maintained the patient database. S.M. and A.R. performed the drug database analysis. Xin W., Xiaochong W. and M.R. provided technical support. R.Y.B.C., A.C., E.C., R.D.C., G.R.H., S.D.J., Y.L., A.L., K.L.M., K.M.N., J.Q.Q., A.G.J.R., N.T., R.J.V., I.B., R.A.M., A.J.M., R.H. and S.J.M.J. led the RNA-Seq and WGS experiments and performed data analyses. A.F.-L. and A.M.K. provided the database of SHH-responsive genes. R.J.W.-R., W.A.G., M.P.-P., C.C.H., O.D., S.S.R., F.F.D., S.S.P.-F., B.-K.C., S.-K.K., K.-C.W., W.S., C.G.E., M.F.-M., A.J., I.F.P., X.F., K.M.M., G.Y.G., C.D.R., L.M., E.M.C.M., N.K.K., P.J.F., J.M.K., J.M.O., R.G.E., K.Z., L.K., R.C.T., M.K.C., B.La., R.E.M., D.D.B., A.F., S.A., N.J., J.C.L., S.B., N.G., W.A.W., L.B., A.K.I., T.E.V.M., T.K., T.T., S.K.E., J.R.L., J.B.R., L.M.L., E.G.V.M., M.F., H.N., G.C., M.G., P.H., A.G.S., A.I., S.J., C.G.C., R.V., Y.S.R., S.R., M.Z., C.C.F., J.A.C., M.L.L., Y.-J.C., U.T., C.E.H., E.B., S.C.C. and S.M.P. provided the patient samples and clinical details that made the study possible. P.H.B.S., M.M., S.L.P., Y.-J.C., U.T., C.E.H., E.B., S.W.S., J.T.R., D.M., S.C.C., S.J.M.J., J.O.K., S.M.P. and M.A.M. provided valuable input regarding study design, data analysis, and interpretation of results. P.A.N., D.J.H.S., J.P., L.G., A.S.M., M.A.M. and M.D.T. wrote the manuscript. M.A.M. and M.D.T. provided financial and technical infrastructure and oversaw the study. M.A.M. and M.D.T. are joint senior authors and project co-leaders.

**Author Information** SNP6 copy number and gene expression array data have been deposited at the Gene Expression Omnibus (GEO; <http://www.ncbi.nlm.nih.gov/geo/>) as a GEO SuperSeries under accession number GSE37385. Whole genome and transcriptome sequencing data have been deposited at the European Genome-phenome Archive (EGA; <https://www.ebi.ac.uk/ega/>) hosted by the EBI, under accession number EGAD00001000158. Reprints and permissions information is available at [www.nature.com/reprints](http://www.nature.com/reprints). This paper is distributed under the terms of the Creative Commons Attribution-Non-Commercial-Share Alike licence, and is freely available to all readers at [www.nature.com/nature](http://www.nature.com/nature). The authors declare no competing financial interests. Readers are welcome to comment on the online version of this article at [www.nature.com/nature](http://www.nature.com/nature). Correspondence and requests for materials should be addressed to M.A.M. ([marram@bcgsc.ca](mailto:marram@bcgsc.ca)) or M.D.T. ([mdtaylor@sickkids.ca](mailto:mdtaylor@sickkids.ca)).

Paul A. Northcott<sup>1,2\*</sup>, David J. H. Shih<sup>1,3\*</sup>, John Peacock<sup>1,3</sup>, Livia Garzia<sup>1</sup>, A. Sorana Morrissy<sup>1</sup>, Thomas Zichner<sup>4</sup>, Adrian M. Stütz<sup>4</sup>, Andrey Korshunov<sup>5</sup>, Jüri Reimand<sup>6</sup>, Steven E. Schumacher<sup>7</sup>, Rameen Beroukhi<sup>7,8,9,10,11,12</sup>, David W. Ellison<sup>13</sup>, Christian R. Marshall<sup>14</sup>, Anath C. Lionel<sup>15</sup>, Stephen Mack<sup>1,3</sup>, Adrian Dubuc<sup>1,3</sup>, Yuan Yao<sup>1,3</sup>, Vijay Ramaswamy<sup>1,3</sup>, Betty Luu<sup>1,3</sup>, Adi Rolider<sup>1</sup>, Florence M. G. Cavalli<sup>1,3</sup>, Xin Wang<sup>1,3</sup>, Marc Remke<sup>1</sup>, Xiaochong Wu<sup>1</sup>, Readman Y. B. Chiu<sup>16</sup>, Andy Chu<sup>16</sup>, Eric Chuah<sup>16</sup>, Richard D. Corbett<sup>16</sup>, Gemma R. Hoad<sup>16</sup>, Shaun D. Jackman<sup>16</sup>, Yisu Li<sup>16</sup>, Allan Lo<sup>16</sup>, Karen L. Mungall<sup>16</sup>, Ka Ming Nip<sup>16</sup>, Jenny Q. Qian<sup>16</sup>, Anthony G. J. Raymond<sup>16</sup>, Nina Thiesen<sup>16</sup>, Richard J. Varhol<sup>16</sup>, Inanc Biroli<sup>16</sup>, Richard A. Moore<sup>16</sup>, Andrew J. Mungall<sup>16</sup>, Robert Holt<sup>17</sup>, Daisuke Kawachi<sup>18</sup>, Martine F. Roussel<sup>18</sup>, Marcel Kool<sup>2</sup>, David T. W. Jones<sup>2</sup>, Hendrick Witt<sup>19,20</sup>, Africa Fernandez-L<sup>21</sup>, Anna M. Kenney<sup>22,23</sup>, Robert J. Wechsler-Reya<sup>24</sup>, Peter Dirks<sup>25</sup>, Tzvi Aviv<sup>26</sup>, Wiesława A. Grajkowska<sup>27</sup>, Marta Perek-Polnik<sup>28</sup>, Christine C. Haberler<sup>29</sup>, Olivier Delattre<sup>30</sup>, Stéphanie S. Reynaud<sup>31</sup>, François F. Doz<sup>32</sup>, Sarah S. Pernet-Fattet<sup>33</sup>, Byung-Kyu Cho<sup>34</sup>, Seung-Ki Kim<sup>34</sup>, Kyu-Chang Wang<sup>34</sup>, Wolfram Scheurlen<sup>35</sup>, Charles G. Eberhart<sup>36</sup>, Michelle Fèvre-Montange<sup>37</sup>, Anne Jouvett<sup>38</sup>, Ian F. Pollack<sup>39</sup>, Xing Fan<sup>40</sup>, Karin M. Muraszko<sup>41</sup>, G. Yancey Gillespie<sup>42</sup>, Concezio Di Rocco<sup>43</sup>, Luca Massimi<sup>43</sup>, Erna M. C. Michiels<sup>44</sup>, Nanne K. Kloosterhof<sup>44,45</sup>, Pim J. French<sup>45</sup>, Johan M. Kros<sup>46</sup>, James M. Olson<sup>47,48</sup>, Richard G. Ellenbogen<sup>49</sup>, Karel Zitterbart<sup>50,51</sup>, Leos Kren<sup>52</sup>, Reid C. Thompson<sup>22</sup>, Michael K. Cooper<sup>53</sup>, Boleslaw Lach<sup>54,55</sup>, Roger E. McLendon<sup>56</sup>, Darel D. Bigner<sup>56</sup>, Adam Fontebasso<sup>57</sup>, Steffen Albrecht<sup>58,59</sup>, Nada Jabado<sup>57,60</sup>, Janet C. Lindsey<sup>61</sup>, Simon Bailey<sup>61</sup>, Nalin Gupta<sup>62</sup>, William A. Weiss<sup>63</sup>, László Bognár<sup>64</sup>, Almos Klekner<sup>64</sup>, Timothy E. Van Meter<sup>65</sup>, Toshihiro Kumabe<sup>66</sup>, Teiji Tominaga<sup>66</sup>, Samer K. Elbaba<sup>67</sup>, Jeffrey R. Leonard<sup>68</sup>, Joshua B. Rubin<sup>69</sup>, Linda M. Liau<sup>70</sup>, Erwin G. Van Meir<sup>71</sup>, Maryam Fouladi<sup>72</sup>, Hideo Nakamura<sup>73</sup>, Giuseppe Cinalli<sup>74</sup>, Miklós Garami<sup>75</sup>, Peter Hauser<sup>75</sup>, Ali G. Saad<sup>76</sup>, Achille Iolascon<sup>77,78</sup>, Shin Jung<sup>79</sup>, Carlos G. Carlotti<sup>80</sup>, Rajeev Vibhakari<sup>81</sup>, Young Shin Ra<sup>82</sup>, Shenandoah Robinson<sup>83,84</sup>, Massimo Zollo<sup>77,78</sup>, Claudia C. Faria<sup>85,86</sup>, Jennifer A. Chan<sup>87</sup>, Michael L. Levy<sup>88</sup>, Poul H. B. Sorensen<sup>89</sup>, Matthew Meyerson<sup>9</sup>, Scott L. Pomeroy<sup>90</sup>, Yoon-Jae Cho<sup>91</sup>, Gary D. Bader<sup>6,14,92,93</sup>, Uri Tabori<sup>94</sup>, Cynthia E. Hawkins<sup>95</sup>, Eric Bouffet<sup>94</sup>, Stephen W. Scherer<sup>14,15</sup>, James T. Rutka<sup>25</sup>, David

Malkin<sup>94,96</sup>, Steven C. Clifford<sup>61</sup>, Steven J. M. Jones<sup>16</sup>, Jan O. Korbel<sup>4</sup>, Stefan M. Pfister<sup>2,19</sup>, Marco A. Marra<sup>17,97</sup> & Michael D. Taylor<sup>1,3,25</sup>

<sup>1</sup>Developmental & Stem Cell Biology Program, The Hospital for Sick Children, 101 College Street, TMDT-11-401M, Toronto, Ontario M5G 1L7, Canada. <sup>2</sup>Division of Pediatric Neurooncology, German Cancer Research Center (DKFZ), Im Neuenheimer Feld 280, 69120 Heidelberg, Germany. <sup>3</sup>Department of Laboratory Medicine and Pathobiology, University of Toronto, Medical Sciences Buildings, 1 King's College Circle, 6th Floor, Toronto, Ontario M5S 1A8, Canada. <sup>4</sup>Genome Biology, European Molecular Biology Laboratory, Meyerhofstrasse 1, 69117 Heidelberg, Germany. <sup>5</sup>CCU Neuropathology, German Cancer Research Center (DKFZ), Im Neuenheimer Feld 220-221, Department of Neuropathology, University of Heidelberg, Im Neuenheimer Feld 224, 69120 Heidelberg, Germany. <sup>6</sup>The Donnelly Centre, University of Toronto, 160 College Street, Room 602, Toronto, Ontario M5S 3E1, Canada. <sup>7</sup>Department of Cancer Biology, Dana-Farber Cancer Institute, 450 Brookline Avenue, Boston, Massachusetts 02215, USA. <sup>8</sup>Department of Medical Oncology, Dana-Farber Cancer Institute, 450 Brookline Avenue, Boston, Massachusetts 02215, USA. <sup>9</sup>Department of Medicine, Harvard Medical School, 25 Shattuck Street, Boston, Massachusetts 02115, USA. <sup>10</sup>Department of Medicine, Brigham and Women's Hospital, 75 Francis Street, Boston, Massachusetts 02115, USA. <sup>11</sup>Cancer Program, Broad Institute, 7 Cambridge Center, Cambridge, Massachusetts 02142, USA. <sup>12</sup>Center for Cancer Genome Discovery, Dana-Farber Cancer Institute, 450 Brookline Avenue, Boston, Massachusetts 02215, USA. <sup>13</sup>Pathology, St Jude Children's Research Hospital, 262 Danny Thomas Place, Memphis, Tennessee 38105, USA. <sup>14</sup>McLaughlin Centre and Department of Molecular Genetics, University of Toronto, 101 College Street, Toronto, Ontario M5G 1L7, Canada. <sup>15</sup>The Centre for Applied Genomics and Program in Genetics and Genome Biology, The Hospital for Sick Children, 101 College Street, TMDT-14-701, Toronto, Ontario M5G 1L7, Canada. <sup>16</sup>Michael Smith Genome Sciences Centre, BC Cancer Agency, 100-570 West 7th Avenue, Vancouver, British Columbia V5Z 4S6, Canada. <sup>17</sup>Michael Smith Genome Sciences Centre, BC Cancer Agency, 675 West 10th Avenue, Vancouver, British Columbia V5Z 1L3, Canada. <sup>18</sup>Tumour Cell Biology, St Jude Children's Research Hospital, 262 Danny Thomas Place, Memphis, Tennessee 38105, USA. <sup>19</sup>Department of Pediatric Oncology, University Hospital Heidelberg, Im Neuenheimer Feld 430, 69120 Heidelberg, Germany. <sup>20</sup>Departments of Hematology and Immunology, University Hospital Heidelberg, Im Neuenheimer Feld 430, 69120 Heidelberg, Germany. <sup>21</sup>Pediatric Clinical Trials Office, Memorial Sloan-Kettering Cancer Center, 405 Lexington Avenue, New York, New York 10174, USA. <sup>22</sup>Neurological Surgery, Vanderbilt Medical Center, T-4224 MCN, Nashville, Tennessee 37232-2380, USA. <sup>23</sup>Cancer Biology, Vanderbilt Medical Center, 465 21st Avenue South, MRB III 6160, Nashville, Tennessee 37232-8550, USA. <sup>24</sup>Sanford-Burnham Medical Research Institute, La Jolla, California 92037, USA. <sup>25</sup>Department of Surgery, Division of Neurosurgery and Labatt Brain Tumour Research Centre, The Hospital for Sick Children, 555 University Avenue, Hill 1503, Toronto, Ontario M5G 1X8, Canada. <sup>26</sup>Developmental & Stem Cell Biology Program, The Hospital for Sick Children, 101 College Street, TMDT-13-601, Toronto, Ontario M5G 1L7, Canada. <sup>27</sup>Department of Pathology, The Children's Memorial Health Institute, Aleja Dzieci Polskich 20, 04-730 Warsaw, Poland. <sup>28</sup>Department of Oncology, The Children's Memorial Health Institute, Aleja Dzieci Polskich 20, 04-730 Warsaw, Poland. <sup>29</sup>Institute of Neurology, Medical University of Vienna, AKH 4J, Waehringer Gürtel 18-20, A-1097 Vienna, Austria. <sup>30</sup>INSERM U 830, Institut Curie, 26 rue d'Ulm, 75238 Paris Cedex 5, France. <sup>31</sup>Unit of Somatic Genetics, Institut Curie, 26 rue d'Ulm, 75238 Paris Cedex 5, France. <sup>32</sup>Department of Pediatric Oncology, Institut Curie, 26 rue d'Ulm, 75248 Paris Cedex 5, France. <sup>33</sup>Pediatric Hematology and Oncology, CHUV University Hospital, 1011 Lausanne, Switzerland. <sup>34</sup>Department of Neurosurgery, Division of Pediatric Neurosurgery, Seoul National University Children's Hospital, 101 Daehak-Ro Jongno-Gu, Seoul 110-744, South Korea. <sup>35</sup>Head of Pediatrics, Cnopfsche Kinderklinik, Theodor-Kutzer-Ufer 1-3, 90419 Nuremberg, Germany. <sup>36</sup>Departments of Pathology, Ophthalmology and Oncology, John Hopkins University School of Medicine, 720 Rutland Avenue, Ross Building 558, Baltimore, Maryland 21205, USA. <sup>37</sup>INSERM U1028, CNRS UMR5292, Centre de Recherche en Neurosciences, Université de Lyon, 69336 Lyon, France. <sup>38</sup>Centre de Pathologie EST, Groupement Hospitalier EST, Université de Lyon, 69500 Bron, France. <sup>39</sup>Department of Neurological Surgery, University of Pittsburgh School of Medicine, 4401 Penn Avenue, Pittsburgh, Pennsylvania 15224, USA. <sup>40</sup>Departments of Neurosurgery and Cell and Developmental Biology, University of Michigan Medical School, 109 Zina Pitcher Place, 5018 BSRB, Ann Arbor, Michigan 48109, USA. <sup>41</sup>Department of Neurosurgery, University of Michigan Medical School, 1500 E. Medical Center Drive, Taubman Center, Room 3552, Ann Arbor, Michigan 48109, USA. <sup>42</sup>Department of Surgery, Division of Neurosurgery, University of Alabama at Birmingham, 1900 University Boulevard, THT 1052, Birmingham, Alabama 35294-0006, USA. <sup>43</sup>Pediatric Neurosurgery, Catholic University Medical School, 00186 Rome, Italy. <sup>44</sup>Department of Pediatric Oncology and Hematology, Erasmus Medical Center, Dr. Molewaterplein 50, 3000 Rotterdam, The Netherlands. <sup>45</sup>Department of Neurology, Erasmus Medical Center, Dr. Molewaterplein 50, PO Box 2040, 3000 CA Rotterdam, The Netherlands. <sup>46</sup>Department of Pathology, Erasmus Medical Center, Dr. Molewaterplein 50, 3015 GE Rotterdam, The Netherlands. <sup>47</sup>Clinical Research Division, Fred Hutchinson Cancer Research Center, 1100 Fairview Avenue North, D4-100, Seattle, Washington 98109, USA. <sup>48</sup>Seattle Children's Hospital, Seattle, Washington 98104, USA. <sup>49</sup>Neurological Surgery, University of Washington School of Medicine, Harborview Medical Center, 325 Ninth Avenue, Seattle, Washington 98104, USA. <sup>50</sup>Department of Pediatric Oncology, School of Medicine, Masaryk University, Cernoplni 9, 613 00 Brno, Czech Republic. <sup>51</sup>Department of Pediatric Oncology, University Hospital Brno, 625 00 Brno, Czech Republic. <sup>52</sup>Department of Pathology, University Hospital Brno, Jihlavská 20, 625 00 Brno, Czech Republic. <sup>53</sup>Department of Neurology, Vanderbilt Medical Center, 465 21st Avenue South, MRB III 6160, Nashville, Tennessee 37232-8550, USA. <sup>54</sup>Department of Pathology and Molecular Medicine, Division of Anatomical Pathology, McMaster University, Hamilton, Ontario L8S 4L8, Canada. <sup>55</sup>Department of Pathology and Laboratory Medicine, Hamilton General Hospital, 237 Barton Street East, Hamilton, Ontario L8L 2X2, Canada. <sup>56</sup>Department of Pathology, Duke University, DUMC 3712,

Durham, North Carolina 27710, USA.<sup>57</sup>Division of Experimental Medicine, McGill University, 4060 Ste Catherine West, Montreal, Quebec H3Z 2Z3, Canada.<sup>58</sup>Department of Pathology, McGill University, Montreal, Quebec H3A 2B4, Canada.<sup>59</sup>Department of Pathology, Montreal Children's Hospital, 2300 Tupper, Montreal, Quebec H3H 1P3, Canada.<sup>60</sup>Department of Pediatrics, Division of Hemato-Oncology, McGill University, Montreal, Quebec H3H 1P3, Canada.<sup>61</sup>Northern Institute for Cancer Research, Newcastle University, Newcastle upon Tyne NE1 4LP, United Kingdom.<sup>62</sup>Departments of Neurological Surgery and Pediatrics, University of California San Francisco, 505 Parnassus Avenue, Room M779, San Francisco, California 94143-0112, USA.<sup>63</sup>Departments of Neurology, Pediatrics, and Neurosurgery, University of California San Francisco, The Helen Diller Family Cancer Research Building 1450 3rd Street, Room HD-220, MC0520, San Francisco, California 94158, USA.<sup>64</sup>Department of Neurosurgery, University of Debrecen, Medical and Health Science Centre, Móricz Zs. Krt. 22., 4032 Debrecen, Hungary.<sup>65</sup>Pediatrics, Virginia Commonwealth University, School of Medicine, Box 980646, Pediatric Hematology-Oncology, 1101 East Marshall Street, Richmond, Virginia 23298-0646, USA.<sup>66</sup>Department of Neurosurgery, Tohoku University Graduate School of Medicine, 1-1 Seiryō-machi, Aoba-ku, Sendai 980-8574, Japan.<sup>67</sup>Department of Neurosurgery, Division of Pediatric Neurosurgery, St Louis University School of Medicine, 1465 South Grand Boulevard, Suite 3707, St Louis, Missouri 63104, USA.<sup>68</sup>Department of Neurosurgery, Division of Pediatric Neurosurgery, Washington University School of Medicine and St Louis Children's Hospital, Campus Box 8057, 660 South Euclid Avenue, St Louis, Missouri 63110, USA.<sup>69</sup>Departments of Pediatrics, Anatomy and Neurobiology, Washington University School of Medicine and St Louis Children's Hospital, Campus Box 8208, 660 South Euclid Avenue, St Louis, Missouri 63110, USA.<sup>70</sup>Department of Neurosurgery, David Geffen School of Medicine at UCLA, 10833 Le Conte Avenue, Campus 690118, Los Angeles, California 90095, USA.<sup>71</sup>Laboratory of Molecular Neuro-Oncology, Departments of Neurosurgery and Hematology & Medical Oncology, School of Medicine and Winship Cancer Institute, Emory University, 1365C Clifton Road NE, Atlanta, Georgia 30322, USA.<sup>72</sup>Division of Oncology, University of Cincinnati, Cincinnati Children's Hospital Medical Center, Cincinnati, Ohio 45229, USA.<sup>73</sup>Department of Neurosurgery, Kumamoto University Graduate School of Medical Science, 1-1-1, Honjo, Kumamoto 860-8556, Japan.<sup>74</sup>Paediatric Neurosurgery, Ospedale Santobono-Pausilipon, 80145 Naples, Italy.<sup>75</sup>2nd Department of Pediatrics, Semmelweis University, 1085 Budapest, Hungary.<sup>76</sup>Pathology, University of Arkansas for

Medical Sciences, 1 Children's Way, lot 820, Little Rock, Arkansas 72202, USA.<sup>77</sup>Dipartimento di Biochimica e Biotecnologie Mediche, University of Naples, Via Pansini 5, 80145 Naples, Italy.<sup>78</sup>CEINGE Biotecnologie Avanzate, Via Gaetano Salvatore 486, 80145 Naples, Italy.<sup>79</sup>Department of Neurosurgery, Chonnam National University Research Institute of Medical Sciences, Chonnam National University Hwasun Hospital and Medical School, 322 Seoyang-ro, Hwasun-eup, Hwasun-gun, Chonnam 519-763, South Korea.<sup>80</sup>Department of Surgery and Anatomy, Faculty of Medicine of Ribeirão Preto, Universidade de São Paulo, Brazil, Avenida Bandeirantes, 3900, Monte Alegre, 14049-900, Rebeirao Preto, São Paulo, Brazil.<sup>81</sup>Pediatrics, University of Colorado Denver, 12800 19th Avenue, Aurora, Colorado 80045, USA.<sup>82</sup>Department of Neurosurgery, University of Ulsan, Asan Medical Center, Seoul, 138-736, South Korea.<sup>83</sup>Division of Pediatric Neurosurgery, Case Western Reserve, Cleveland, Ohio 44106, USA.<sup>84</sup>Rainbow Babies & Children's, Cleveland, Ohio 44106, USA.<sup>85</sup>Division of Neurosurgery, Hospital de Santa Maria, Centro Hospitalar Lisboa Norte EPE, 1169-050, Lisbon, Portugal.<sup>86</sup>Cell Biology Program, The Hospital for Sick Children, 101 College Street, TMDT-401-J, Toronto, Ontario M5G 1L7, Canada.<sup>87</sup>Department of Pathology and Laboratory Medicine, University of Calgary, 3330 Hospital Drive NW, HRIC 2A25A, Calgary, Alberta T2N 4N1, Canada.<sup>88</sup>UCSD Division of Neurosurgery, Rady Children's Hospital San Diego, 8010 Frost Street, Suite 502, San Diego, California 92123, USA.<sup>89</sup>Department of Molecular Oncology, British Columbia Cancer Research Centre, 675 West 10th Avenue, Vancouver, British Columbia V5Z 1L3, Canada.<sup>90</sup>Department of Neurology, Harvard Medical School, Children's Hospital Boston, Fegan 11, 300 Longwood Avenue, Boston, Massachusetts 02115, USA.<sup>91</sup>Department of Neurology and Neurological Sciences, Stanford University School of Medicine, 1201 Welch Road, MSLS Building, Rm P213, Stanford, California 94305, USA.<sup>92</sup>Banting and Best Department of Medical Research, University of Toronto, Toronto, Ontario M5G 1L6, Canada.<sup>93</sup>Samuel Lunenfeld Research Institute at Mount Sinai Hospital, University of Toronto, Toronto M5G 1X5, Ontario, Canada.<sup>94</sup>Department of Haematology & Oncology, The Hospital for Sick Children, 555 University Avenue, Toronto, Ontario M5G 1X8, Canada.<sup>95</sup>Department of Pathology, The Hospital for Sick Children, 555 University Avenue, Toronto, Ontario M5G 1X8, Canada.<sup>96</sup>Department of Pediatrics, University of Toronto, Toronto, Ontario M5G 1X8, Canada.<sup>97</sup>Department of Medical Genetics, University of British Columbia, 675 West 10th Avenue, Vancouver, British Columbia V5Z 1L3, Canada.

\*These authors contributed equally to this work.